論 文
35~8~7

6펄스 콘버어터로 제어되는 초전도에너지 저장장치에 의한 전력계통 안정화

Power System Stabilization by Superconducting Magnet Energy Storage (SMES) Controlled by 6 Pulse Converter

車 貴 守* · 韓 松 曄** · 元 鍾 洙**
(Guee-Soo Cha · Song-Yop Hahn · Jong-Soo Won)

요 약

전력계통의 안정도 향상 및 전압동요억제용으로 사용되는 초전도 에너지저장장치를 제어하기 위해 일반적으로 사용되는 12펄스 콘버어터를 대신해서 6펄스 콘버어터를 사용할 수 있음을 보였다. 유효전력과 무효전력의 동시제어를 위해서 6펄스 콘버어터를 비대칭으로 제어했을 때 문제가 되는 전류실패를 방지하기 위해서, 전류 임계점에서의 전류현상을 해석함으로 안정제어 영역을 구했다. 또한 비대칭제어시에 발생하는 선전류 및 부하전압의 고조파 성분을 구했다. 본 연구에서 제시된 비대칭제어 방식에 의한 전력계통 안정화를 컴퓨터 시뮬레이션을 통해 보임으로서 본 방식의 효용성을 입증했다. 결과에 의하면 동요발생 및 과도상태 발생시에 6펄스 콘버어터로 제어되는 초전도 에너지저장장치가 전력계통의 안정도를 향상시키는데 효과적인 것으로 밝혀졌다.

Abstract

This paper shows that 6 pulse converter instead of 12 pulse converter can be used for the control of Superconducting Magnet Energy Storage(SMES) to improve the stability and to suppress the voltage fluctuation of power system. In order to prevent the commmutationn failure, when 6 pulse converter used for simultaneous control of real power and reactive power is asymmetrically controlled, stable control region has been presented by analyzing the commutation phenomena at critical points which distinguish the stable control region from the unstrol control region. Harmonic components of line current and output voltage have been calculated. Finally, computer simulation of power system stabilization has been presented to show the effectiveness of the proposed method. According to the computation results, SMES controlled by the 6 pulse converter is an effective measure in reducing the oscillation and the transient instability of the power system.

*正 會 員 : 서울大 大學院 電氣工學科 博士課程
**正 會 員 : 서울大 工大 電氣工學科 敎授
接受日字 : 1986年 4月 3日

1. Introduction

Superconducting Magnet Energy Strorage(SM

ES) is an effective measure as an energy storage, where the electrical energy is stored in the form of magnetic energy by current flowing through superconducting magent. The SMES is connected to the power system by thyristorized converter. Because there is no mechanical part and low loss when SMES absorbs or discharges energy, high efficiency and fast response during adsorbing and discharging the energy can be obtained by SMES.[1] By these characteristics, SMES can afford high damping effect and constant line voltage of power system.[2]

In order to increase the stability and to suppress the voltage fluctuation of power system by SMES, the real power (P) and reactive power (Q) must be supplied simultaneously from SMES to power system through the thyristorized power converter.[3] For simultaneous control of P and Q, symmetrically controlled 12 pulse converter,where upper and lower thyristor groups are fired symmetrically, has been conventionally used. But asymmetrically controlled 6 pulse converter,where each thyristor group is fired at different firing angle, can be applied to the simultaneous control of P and Q. At this case, the number of transformers and thyristors reduces to one half.

Asymmetrical control was originally designated in order to minimize the reactive power.[4] For that purpose, one thyristor group was fired at fully advanced (or retarded), the other thyristor group was phase controlled to give the desired output. This method is known to have shortcomings such as third harmonic output ripple, second harmonic line current distortion and danger of commutation failure.[5),6)]

In this paper, asymmetrical contorl theory is expanded to control P and Q simultaneousely. Stable control region where commutation failure dose not occur is found, so that danger of commutation failure which is the most undesirable feature at asymmetrical control and reduction of operational reliability due to it are overcomed. Computer simulation of model power system is done in order to show the effectiveness of the proposed method.

2. Commutation Phenomena

In Fig. 1, energy stored in superconducting coil is controlled by the 6 pulse converter. There is an unique commutation phenomena when asymmetrical firing is applied to 6 pulse converter. Assume Th. 3 or Th. 4 begins to conduct while Th. 1 and Th. 2 are conducting. Commutation phenomena can be divided in two cases as follows, 1) when commutation interference does not exist 2) when commutation interference exists.

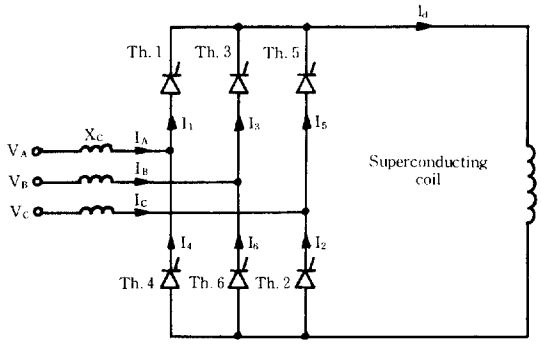

Fig. 1. 6 Pulse converter and superconducting coil connected to the power system.

2.1 Commutation without Commutation Interference

When upper or lower thyrister begins to commutate while Th. 1 and Th. 2 are conducting, time interval where commutation interference between upper and lower thyristors does not take plece is.

$$\alpha_1+u_1+\omega t_{off}>\alpha_2+\frac{\pi}{3} \quad (1)$$

$$\alpha_2+\frac{\pi}{3}+u_2+\omega t_{off}>\alpha_1 \quad (2)$$

where α_i : firing angle of upper and lower thyristor group i=1, 2

μ_i : commutation overlap angle of upper and lower thyristor group i=1, 2

t_{off} : thyristor turn-off time

The phase relation between the firing angle α_1, α_2 and phase voltage is shown in Fig. 2.

In case of no commutation interference, currents of thyristors Th. 1, Th. 2, Th. 3 and Th. 4

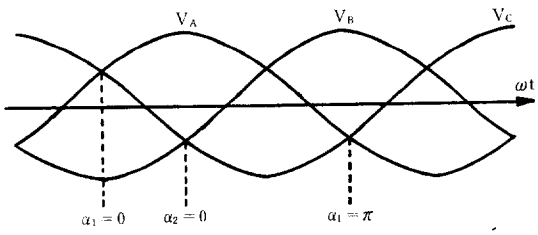

Fig. 2. Phase relation between the firing angle and the phase voltage.

which participate the commutation and load voltage are shown in Fig. 3. Upper thyristors commutate prior to the lower thyristor's commutation in Fig. 3. a) and vice versa in Fig.3.b). When Th.4 begins to commutate prior to Th.2, superconducting coil current I_d freewheels through Th. 1 and Th. 4, therefore, load voltage falls to zero as shown in the load voltage of Fig. 3. b). Let V_P V_n, V_1, V_2, V_3 and V_4 be cathode voltage of upper thyristors, anode voltage of lower thyristors, forward blocking voltage of Th.1, Th. 2, Th.3 and Th.4, respectively. When upper thyristors begin to commutate first, that is, Th. 3 is fired first,

$$V_P=\frac{1}{2}(V_A+V_B),\quad V_N=V_c \tag{3}$$

$$v_1=v_2=v_3=0,\quad v_4=-3/2V_c \tag{4}$$

$$I_3=\frac{1}{X_c}\int_{\alpha 1}^{\alpha 1+u1}\frac{1}{2}(V_A-V_B)d(\omega t) \tag{5}$$

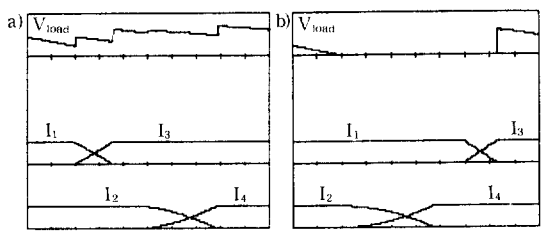

a) commutation between upper thyristors takes place first
$\alpha_1=40°$, $\alpha_2=10°$, $X_c=0.2$pu
b) commutation between lower thyristors takes place first
$\alpha_1=110°$, $\alpha_2=10°$, $X_c=0.2$pu

Fig. 3. Current transfer between thyristor, without commutation interference.

If lower thyristors start to commutate first, that is, Th.4 is fired first,

$$V_P=\frac{1}{2}(V_A+V_C),\quad V_N=V_P \tag{6}$$

$$v_1=v_2=v_4=0,\quad v_3=3/2\,V_B \tag{7}$$

$$I_4=\frac{1}{X_c}\int_{\alpha 2+\frac{\pi}{3}}^{\alpha 2+\frac{\pi}{3}+u2}\frac{1}{2}(V_A-V_C)d(\omega t) \tag{8}$$

2.2 Commutation with commutation interference

Time interval where commutation interference takes place can be expressed as

$$\alpha_1+u_1+\omega t_{off}<\alpha_2+\frac{\pi}{3} \tag{9}$$

$$\alpha_2+\frac{\pi}{3}+u_2+\omega t_{off}<\alpha_1 \tag{10}$$

When lower thyristors Th. 2 and Th. 4 commence to commutate while upper thyristors Th. 1 and Th. 3 are commutating, commutation phenomena can be formulated as

$$V_P=0\quad V_N=0 \tag{11}$$

$$v_1=v_2=v_3=v_4=0 \tag{12}$$

$$I_3=\frac{1}{X_c}\int_{\alpha 2+\frac{\pi}{3}}^{\beta}V_A\,d(\omega t) \tag{13}$$

$$I_4=\frac{1}{X_c}\int_{\alpha 2+\frac{\pi}{3}}^{\beta}V_c\,d(\omega t) \tag{14}$$

where β : extinction angle where commutation of one thyristor group is finished.

As seen in Eqs. 11)--14), commutation with commutation interference shows different feature from commutation without commutation interference. Duration of each thyristor group's commutation may increase or decrease by this commutation interference. If

$$\alpha_1+u_1<\frac{5}{6}\pi \tag{15}$$

retriggering of commutated upper thyristor does not occur though lower thyristors begin to commutate within the lapse of turn-off time because negative forward blocking voltage is applied to the thyristor just commutated.

When upper thyristors Th.1 and Th.3 commence to commutate while lower thyristors Th. 2 and Th.4 are commutating, Eqs. 11)--14) are va-

lid except the substitution of α_1 for $\alpha_2+\frac{\pi}{3}$. And if

$$\alpha_2+u_2<\frac{\pi}{6} \tag{16}$$

retriggering of commutated lower thyristor does not occur because of the same reason as above. Eqs. 11)--14) are still valid when upper and lower thyristors start to commutate simultaneously, $\alpha_1=\alpha_2+\frac{\pi}{6}$, until one thyristor group completes the commutation. Fig.4. a) shows commencement of lower thyristor group's commutation during upper thyristor group's commutation and Fig. 4. b) shows simultaneous commencement of upper and lower thyristor group's commutation.

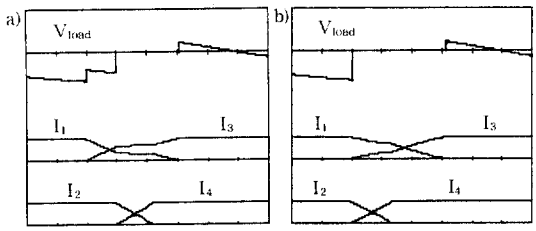

a) commencement of lower thyristor's commutation during upper thyristor's commutation
$\alpha_1=130°$, $\alpha_2=70°$, $X_c=0.2$pu
b) simultaneous commencement of upper and lower thyristor's commutation
$\alpha_1=130°$, $\alpha_2=70°$, $X_c=0.2$pu

Fig. 4. Current transfer between thyristors, with commutation interference.

At asymmetrical control, thyristor fired may not start to conduct. When Th. 4 is fired within $\alpha_2<\pi/6$ while upper thyristors are commutating, Th. 4 cannot commence to commutate because i_4 is negative according to Eq. 14). Th. 4 can start to conduct at $wt=\pi/6$ or after the completion of upper thyristor group's commutation where i_4 becomes positive. If Th. 3 is fired at $\alpha_1>5\pi/6$ while lower thyristors are commutating, conduction of Th. 3 is delayed as the same reason above until commutation of lower thyristor group is finished.

Fig. 5 shows the converter phase voltage, load vo-

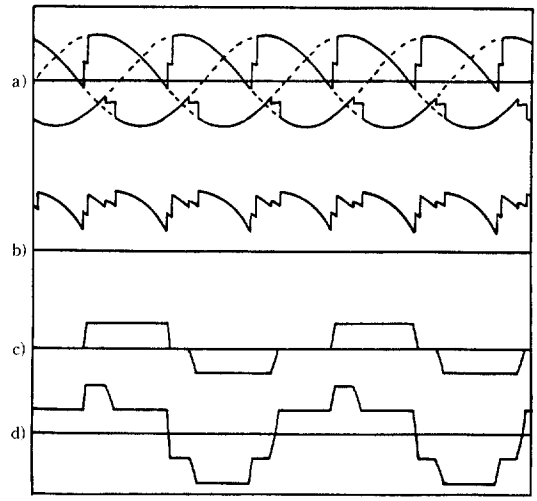

a) phase voltage
b) load voltage
c) secondary current of transformer
d) primary current of transformer

Fig. 5. Commutation phenomena with no commutation interference, $\alpha_1=40°$, $\alpha_2=10°$, $X_c=0.05$pu.

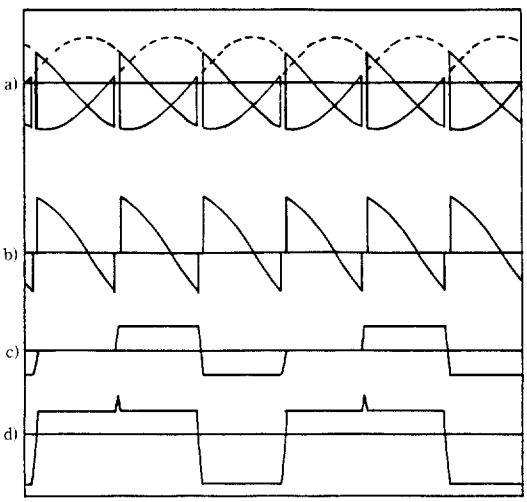

a)-d) : the same as in Fig. 5

Fig. 6. Commutation phenomena at simultaneous commencement of upper and lower thyristors, $\alpha_1=100°$, $\alpha_2=40°$, $X_c=0.05$pu.

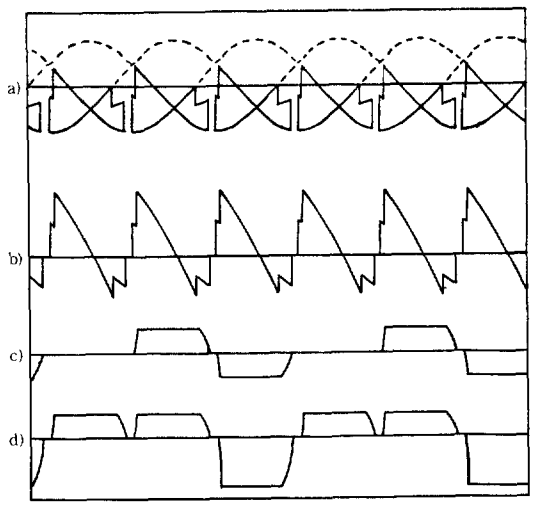

a)-d) : the same as in Fig. 5

Fig. 7. Commutation phenomena having $\pi/6$ freewheeling interval, $\alpha_1=120°$, $\alpha_2=30°$, $X_c=0.05$pu.

ltage, second and primary line current of transformer where commutation interference does not exist. Converter is assumed to be linked to the power system via transformer connected in delta-wye. Simultaneous commencement of upper and lower thyristor group's commutation, $\alpha_1=\alpha_2+\pi/3$, is represented in Fig. 6 and an example of freewheeling during $\pi/6$ through Th. 1 and Th.4 is shown in Fig. 7.

3. Maximum Control Angle

Simultaneous commutation of upper and lower thyristor group can take place in asymmetrically controlled converter. At this case, maximum control angle α_{max} is different from that of symmetrically controlled converter because both groups are influenced by each other.

If there is no commutation interference, α_{max} is the same as that of symmetrical control. If Th. 3 is fired while Th. 1 and Th. 2 are conducting,

$$I_3=\frac{1}{X_c}\int_{\alpha_{max}}^{\pi-t_{off}}[V_B-\tfrac{1}{2}(V_A+V_B)]d(\omega t)=I_d \tag{17}$$

and α_{max} is given as follows

$$\alpha_{max}=\cos^{-1}\left[\frac{\sqrt{2}X_c}{\sqrt{3}V}I_d-\cos(\omega t_{off})\right] \tag{18}$$

In case of commutation inteference, commutation critical points which distinguish stable control region from unstable control region can be classified into five cases as follows.

a) $\alpha_1=\alpha_2+u_2+\frac{\pi}{3}$, $\alpha_1=\alpha_{max}$

Th. 4 is fired while Th. 1 and Th. 2 are conducting, so that commutation of lower thyristors ceases at α_{max} · And Th. 3 is fired at α_{max}. At this case,

$$I_4=\frac{1}{X_c}\int_{\alpha+\frac{\pi}{3}}^{\alpha_{max}}[V_c-\tfrac{1}{2}(V_C+V_A)]d(\omega t)=I_d \tag{19}$$

From above equation, α_2 is given by the following equation

$$\alpha_2=\cos^{-1}\left[\frac{\sqrt{2}X_c}{\sqrt{3}V}I_d+\cos\left(\alpha_{max}-\frac{\pi}{3}\right)\right] \tag{20}$$

b) $\alpha_1=\alpha_2+\frac{\pi}{3}$

Let the Th.2's extinction angle be β, then

$$I_3=\frac{1}{X_c}\int_{\alpha_1}^{\beta}V_B d(\omega t)+\frac{1}{X_c}\int_{\beta}^{\pi-\omega t_{off}}[V_B-\tfrac{1}{2}(V_A+V_B)]d(\omega t)=I_d \tag{21}$$

$$I_4=\frac{1}{X_c}\int_{\alpha_1}^{\beta}V_C d(\omega t)=I_d \tag{22}$$

β can be obtained as follows

$$\beta=\cos^{-1}\left[\cos\left(\alpha-\frac{\pi}{2}\right)-\frac{X_c}{\sqrt{2}V}I_d\right]+\frac{\pi}{2} \tag{23}$$

Inserting β to Eq. 21), then

$$\alpha_1=\cos^{-1}\left[\frac{\sqrt{3}X_c}{\sqrt{2}V}I_d-\cos(\omega t_{off})\right] \tag{24}$$

$$\alpha_2=\alpha_1-\frac{\pi}{3} \tag{25}$$

c) $\alpha_1+u_1=\alpha_2+\frac{\pi}{3}$

Lower thyristor Th. 4 is fired just after the complete commution of upper thyristor Th. 1,thus Th. 1 retriggers.

β of this case is equivalent to Eq. 23) and

$$I_4=\frac{1}{X_c}\int_{\alpha_2+\frac{\pi}{3}}^{\beta}V_C\,d(\omega t)=I_d \tag{26}$$

$$I_3=\frac{1}{X_c}\int_{\alpha_2+\frac{\pi}{3}}^{\beta}V_B\,d(\omega t)+\frac{1}{X_c}\int_{\beta}^{\pi-t_{off}}[V_B-\tfrac{1}{2}(V_A+V_B)]d(\omega t)=I_d$$

$$=\frac{1}{X_c}\int_{\alpha 1}^{\alpha 2+\frac{\pi}{3}}[V_B-\tfrac{1}{2}(V_A+V_B)]d(\omega t) \quad (27)$$

thus,

$$\alpha_1=\cos^{-1}\left[\frac{\sqrt{2}X_c}{\sqrt{3}V}Id+\cos\left(\alpha_2+\frac{\pi}{3}\right)\right] \quad (28)$$

$$\alpha_2=\cos^{-1}\left[\tfrac{1}{2}\frac{\sqrt{2}X_c}{\sqrt{3}V}I_d-\cos(\omega t_{off})\right] \quad (29)$$

d) $\alpha_1+u_1+\omega t_{off}=\alpha_2+\frac{\pi}{3}$

After the completion of upper thyristor Th. 1's commution, lower thyristor Th. 4 is fired just before the lapse of thyristor turn off time, t_{off}, so that Th. 1 retriggers. Eqs. 26) and 27) are valid at this case, so α_2 is expressed as Eq. 29) and

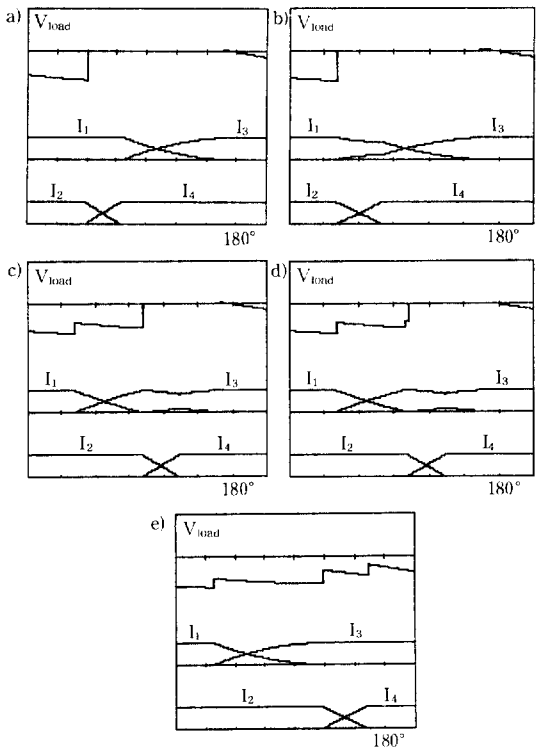

a) $\alpha_1=143.0°$, $\alpha_2=61.1°$
b) $\alpha_1=134.2°$, $\alpha_2=74.0°$
c) $\alpha_1=134.2°$, $\alpha_2=94.0°$
d) $\alpha_1=133.6°$, $\alpha_2=94.0°$
e) $\alpha_1=143.0°$, $\alpha^2=120°$

Fig. 8. Commutation phenomena at critical points, $X_c=0.2$pu.

$$I_3=\frac{1}{X_c}\int_{\alpha 1}^{\alpha_2+\frac{\pi}{3}-\omega t_{off}}[V_B-\tfrac{1}{2}(V_A+V_B)]d(\omega t)=I_d \quad (30)$$

From Eq. 30),

$$\alpha_1=\cos^{-1}\left[\frac{\sqrt{2}X_c}{\sqrt{3}V}I_d+\cos\left(\alpha_2+\frac{\pi}{3}-\omega t_{off}\right)\right] \quad (31)$$

e) $\alpha_1+u_1+\omega t_{off}=\alpha_2+\frac{\pi}{3}$, $\alpha_1=\alpha_{max}$

There is no commution interference at this case because Th. 3 commence to conduct at $\alpha_1=\alpha_{max}$ and Th. 4 at $\alpha_2=2\pi/3$.

Commutation phenomena at the above critical points a)-e)are shown in Fig. 8, where $X_c=0.2$ pu, $I_d=200$A, $V=100$V and $t_{off}=100\mu$s. Considering above conditions synthetically, stable control region where commutation failure doesn't occur can be expressed as in Fig. 9. In Fig. 9. a) and b), X_c is 0.05 pu and X_c is 0.2 pu, respectively, Id, V and t_{off} are the same as in Fig. 8.

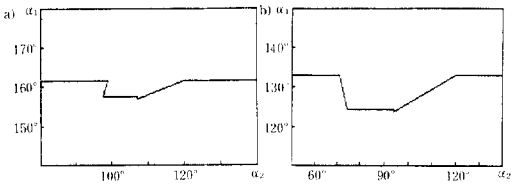

a) $X_c=0.05$pu, $I_d=200$A, $V=100$V and $t_{off}=100\mu$s
b) $X_c=0.2$pu, $I_d=200$A, $V=100$V and $t_{off}=100\mu$s

Fig. 9. Stable control angle

4. Simultaneous Control of Real Power (P) and Reactive Power(Q)

In symmetrical control, P depends on Q and vice versa. Dashed arc A in Fig. 10 represents the control region at symmetrical control. Solid arc B and C are an example of asymmetrical control where one thyristor group is fully advanced (arc B) or fully retarded (arc C) and the other thyristor group is phase controlled in order to give desired output voltage. Futhermore, if upper and lower thyristor group are controlled without any constraint, control region can be expanded to the dashed area in Fig. 10. This means simulta-

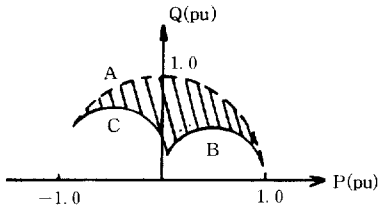

A : control region at symmetrical control
B,C : control region at minimum reactive power control
/// : control region at asymmetrical control

Fig. 10. Control region at $\alpha_{min}=8°$, $\alpha_{max}=150°$.

neous control of P and Q can be realized with 6 pulse converter.

Neglecting the effect of commutation interference first, relation between P, Q and the control angle α_1, α_2 is given as follows.

$$P=\frac{1}{2}E_{d0}\cdot I_d(\cos\theta_1+\cos\theta_2) \quad (32)$$

$$Q=\frac{1}{2}E_{d0}\cdot I_d(\sin\theta_1+\sin\theta_2) \quad (33)$$

where $\cos\theta_1=\cos\alpha_1-\frac{3X_c\cdot I_d}{\pi\cdot E_{d0}}$ (34)

E_{d0} : converter maximum output voltage at no load.

α_1 and α_2 is obtained by Eqs. 32) and 33) as follows

$$\alpha_1=\cos^{-1}\left[\frac{1}{2}\left\{\frac{1}{E_{d0}}\left(\frac{2P}{I_d}+\frac{6X_c}{\pi}I_d\right)+\frac{2Q}{E_{d0}\cdot I_d}\sqrt{\frac{(E_{d0}\cdot I_d)^2}{P^2+Q^2}-1}\right\}\right] \quad (35)$$

$$\alpha_2=\cos^{-1}\left[\frac{1}{2}\left\{\frac{1}{E_{d0}}\left(\frac{2P}{I_d}+\frac{6X_c}{\pi}I_d\right)-\frac{2Q}{E_{d0}\cdot I_d}\sqrt{\frac{(E_{d0}\cdot I_d)^2}{P^2+Q^2}-1}\right\}\right] \quad (36)$$

Effect of commutation interference appears the most remarkably at the critical points a)-e) in

Table. 1. Comparison of the converter output voltage in pu.

	X_c =0.05p.u.		
	Case 1	Case 2	Case 3
a	−0.551	−0.576	−0.576
b	−0.528	−0.553	−0.565
c	−0.609	−0.634	−0.634
d	−0.607	−0.632	−0.631
e	−0.725	−0.750	−0.746

Case 1 : neglecting the commutation overlap and interference
Case 2 : considering the former and neglecting the latter
Case 3 : considering the former and the latter

Fig. 9. Comparison of the three cases; 1) neglecting the commutation overlap and interference, 2) considering the former and neglecting the latter and 3) considering the former and the latter, is shown in Table 1. Maxiumum error due to neglecting the commutation interference is 0.5% at $X_c=0.05$ pu as seen in Table 1. This implys that effect of commutation interference can be neglected and P, Q can be expressed by Eqs. 35)and 36).

5. Harmonic Components

When 6 pulse converter is asymmetrically controlled in order to minimize the reactive power, even harmonics in line current and third multiple of harmonics in load voltage are generated.

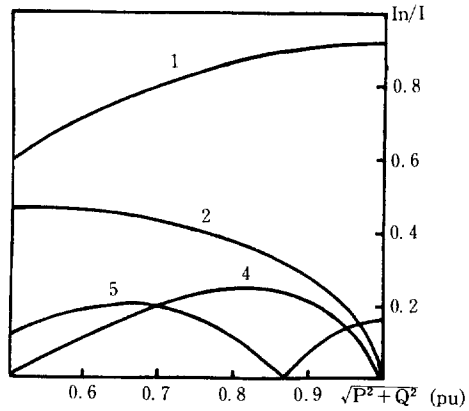

Fig. 11. Harmonic components of transformer primary current while $\sqrt{P^2+Q^2}$ varies from 0.5pu to 1 pu.

The same problems are occurred when asymmetrical control is adopted to contol P and Q simultaneously. Harmonic components of transformer primary current are shown in Fig.11, where apparent power, $\sqrt{P^2+Q^2}$, varies from 0.5 pu to 1.0 pu. Converter is assumed to be linked to the power system via delte-wye connected transformer.

SMES generates only lagging reactive power under the condition of natural commutation, therefore capacitor for power factor correction must be

used in order to generate leading reactive power. Assume the rating of capacitor is 0.7 pu. Fig.12 shows the harmonic component of transformer. primary current at Q=0.7 pu while P is varies from 0.7 pu to −0.7 pu and Fig. 13 shows the harmonic components of load voltage at the same case. The harmonic components presented in a given circuit are multiples of the pulse number in symmetrical control, but third harmonic component exists in asymmetrical control as shown in Fig. 13.

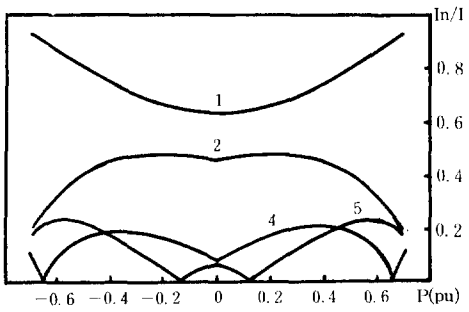

Fig. 12. Harmonic components of transformer primary current at Q=0.7pu.

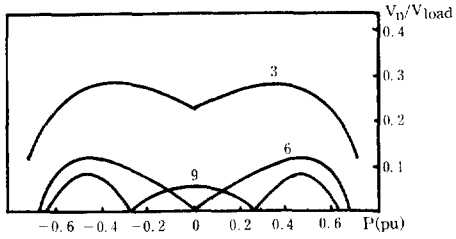

Fig. 13. Harmonic components of load voltage at Q=0.7pu.

Calculation of harmonic components are complexe function of firing angle, commutation overlap and commutation interference. Fast Fourier Transform (FFT) is used to calculate the harmonics.

6. Power System Stabilization by SMES

Two stabilization effects of the SMES are examined by computer simulation of the model power system. One is the suppression of the power system oscillation that aries when one circuit of a double circuit transmission line is opened. The other is the transient stabilizing effect when a three-phase ground fault arises in the transmission line.

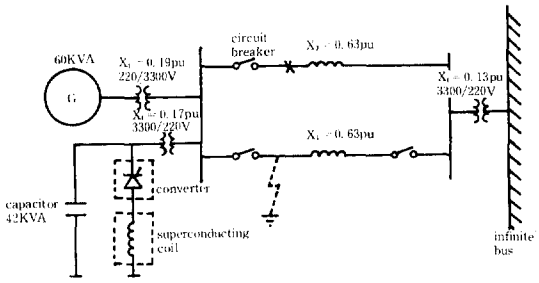

Fig. 14. Configuration of model power system.

Fig. 14 shows the configuration of the model power system. The model power system consists of a 60 KVA synchronous generator connected to an infinite bus via a double circuit transmission line.

Real and rective power of SMES are controlled as follows

$$P=(K_\omega \triangle\omega + K_\delta \triangle\delta)/(1+T_pS) \quad (37)$$

$$Q=(V_{ref}-V_t)/(1+T_qS) \quad (38)$$

where ω : angular speed of generator

δ : generator shaft angular displacement to the infinite bus

T_p, T_q : SMES time constant

AVR characteristics is expressed as follows

$$G=\frac{K(1+T_dS)}{1+T_aS} \quad (39)$$

where K: AVR gain

T_d, T_a: AVR time constant

and generator is formulated using two axis model[7] as follows

$$T_{q0}'\cdot\dot{E}_d'=-\dot{E}_d-(x_q-x_q')I_q \quad (40)$$

$$T_{d0}'\cdot\dot{E}_q'=E_{FD}-E \quad (41)$$

$$\dot{\delta}=\omega-1 \quad (42)$$

$$\dot{\omega}=(P_m-D\omega-P_e)/T_j \quad (43)$$

where E_q' : transient voltage behind q axis
E_d' transient voltage behind d axis
E_{FD} : d axis stator EMF due to V_F
E : stator air gap voltage due to i_F
T_{do}' : d axis open circuit time constant
T_{qo}' : q axis open circuit time constant
X_q : q axis synchronous reactance
X_q' q axis transient reactance
P_m : mechanical input power
P_e : electrical output power
D : damping constant
T_j : inertia constant

Table 2 shows the parameters used in the computer simulation. Fig. 15.a) shows the δ during the oscillation which arises by opening a single circuit. As is apparent from Fig. 15.a), the oscillation is damped within first one wave. Fig.15. b), c) and d) show the P of SMES, Q of SMES and generator terminal voltage, respectively.Fig.

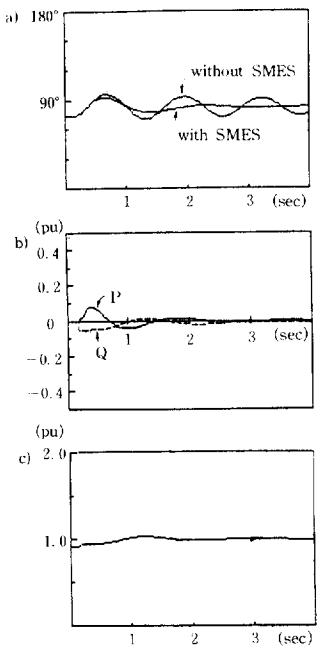

a) angular shaft angle displacement
b) real and imaginary power of SMES
c) generator terminal voltage

Fig. 15. Example of damping improvement by SMES.

Table 2. Parameters used in the computer simulation.

X_d	1.49	(pu)	K=20
$X_{d'}$	0.252	(pu)	T_a=1 (sec)
X_q	0.822	(pu)	T_d=0.2 (sec)
$T_{do'}$	1.56	(sec)	T_p=0.1 (sec)
$T_{qo'}$	0.08	(sec)	T_q=0.1 (sec)
M	7	(sec)	

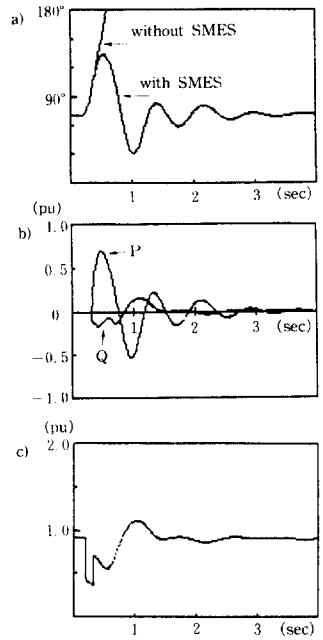

a)-c) ; the same as in Fig. 15.

Fig. 16. Example of transient stability improvement by SMES.

16. shows that generator step out can be prevented by SMES during three phase ground fault. 10 cycle ground fault is assumed in Fig.16. Fig. 16. a)-d) shows the same thing as Fig.15

7. Conclusion

This paper has shown that the real and reactive power can be controlled simultaneously with 6 pulse converter by asymmetrical gating. Commutation phenomena during the asymmetrical

gating has been analyzed and stable control region at this case has been shown. Thus, danger of commutation failure can be avoided.

According to the results, the maximum gating angle of asymmetrically controlled converer decreased silghtly compared to that of symmetrically controlled converter. The proposed 6 pulse converter turned out to be as effective as the 12 pulse converter in reducing the power system transient instability. Power system oscillation was vanished within first wave and step out of synchronous generator was prevented.

Elimination of low order harmonic components in line current and application to multi-machine system are left for future work.

Reference

1) H. A. Peterson, "Superconductive Inductor-Convert Units for Energy Storge in Electric Power system," Proceedings of the International symposium on SCES. 1979
2) H. Kaminosono et al., "Characteristics of Superconducting Magnetic Energy Storage System (SMES) Connected to a Model Power System," IPEC-Tokyo '83, Tokyo, Japan, 1983, pp. 820-830.
3) T. Nitta et al., "Power Charging and Discharging Characteristics of SMES connected to Artificial Transmission Line," IEEE Trans. on MAGN, Vol. MAG-21, No 2,1985, pp.1111-1114
4) W. Mcmurray, "A Study of Asymmetrical Gating for Phase-ControlledConverters,"IEEE Trans. on IA, Vol. IA-8, No.3, 1972, pp. 289-295
5) V.R. Stefanovic, "Power Factor Improvement with Modified Phase Controlled Converter," IEEE Trans. on IA, Vol IA-15 ,No.2,1979,pp. 193-201
6) G. Oliver and Stefanovic, "Thyristor Current Source with an Improved Power Factor,"IEEE Trans. on IE, Vol. IE-29, No, 4, 1982, pp. 299-307
7) P.M. Anderson and A.A. Fouad, Power System Control and Stability, The Iowa State University Press, 1977
8) T. Furuhasi and Y. Amemiya, "A New Firing Method for Improving a Fundamental Input Power Factor in a Modified Phase-Controlled Converter," IPEC-Tokyo '83, Tokyo, Japan, 1983 pp. 1343-1353
9) H.J. Boenig and J.F. Hauer, "Commissioning Tests of the Bonneville Power Administration 30 MJ Superconducting Magnetic Energy Storge Unit, "IEEE Trans.on PAS,Vol. PAS-104, No.2, 1985, pp. 302-312
10) I.M. EI-Amin and A.H.M.A. Rahim, "Stabilization of a High Voltage ACDC Power System II," IEEE Trans. on PAS, Vol. PAS-104, No.11, 1985, pp. 2980-2986.